Estimation and Prediction of Glucose Appearance Rate for Use in a Fully Closed-Loop Dual-Hormone Intraperitoneal Artificial Pancreas

Karim Davari Benam, *Student Member, IEEE,* Sebastien Gros, and Anders Lyngvi Fougner, *Member, IEEE*

***Abstract*—Objective: A fully automated artificial pancreas requires a meal estimator and predictions of blood glucose levels (BGL) to handle disturbances during meal times, all without relying on manual meal announcements and user interventions. This study introduces a technique for estimating the glucose appearance rate (GAR) and predicting BGL in people with type 1 diabetes and insulin and glucagon administration. It is demonstrated for intraperitoneal insulin and glucagon delivery but may be adapted to other delivery sites. Method: The estimator is designed based on the moving horizon estimation (MHE) approach, where the underlying cost function incorporates prior statistical information on the GAR in subjects over the course of a day. The proposed prediction scheme is developed to predict GAR using estimated states and an intestinal model, which is then used to predict BGL with the help of an animal glucose metabolic model. Results: The intraperitoneal dual-hormone estimator was evaluated on three anesthetized animals, achieving a 21.8% mean absolute percentage error (MAPE) for GAR estimation and a 10.0% MAPE for BGL prediction when the future GAR is known. For a 120-minute prediction horizon, the proposed predictor achieved an 18.0% MAPE for GAR and a 28.4% MAPE for BGL. Conclusion: The findings demonstrate the effectiveness and reliability of the proposed estimator and its potential for use in a fully automated artificial pancreas and reducing user interventions. Significance: This study represents advancements toward the development of a fully automated artificial pancreas, ultimately enhancing the quality of life for people with type 1 diabetes.**

***Index Terms*—Artificial pancreas, Continuous glucose monitoring, Diabetes mellitus type 1, Meal estimation, Moving horizon estimation.**

I. Introduction

In people with type 1 diabetes (T1D), the pancreas produces insufficient or no insulin. External insulin delivery is the current approach for these patients to regulate blood glucose levels (BGL). Insulin is a hormone that allows the cells to use glucose as fuel or store it as glycogen. The most common insulin administration method is injecting insulin into the subcutaneous tissue. The amount of insulin required is estimated based on the meal size, activity level, and physical features [1], [2]. The calculation of required insulin can be done by patients or by a control system. A fully automated artificial pancreas (AP) is a system that consists of an infusion pump, a control algorithm, and continuous glucose monitoring (CGM) system that delivers the required insulin automatically without the need for a meal and exercise announcements [3].

Due to the significant time delay in insulin absorption from subcutaneous (SC) tissue, the carbohydrate content of each meal must be announced to the control algorithms in advance to administer a meal-time insulin bolus at the appropriate time [4]. However, estimating the meal size is challenging [5], and patients occasionally forget to announce it to the AP. Unannounced meals can result in high BGL and increase the risk of insulin overdosing in an attempt to decrease the BGL. In addition, any human interventions in the medical control systems are not desired.

Dual-hormone SC APs, which can deliver insulin and glucagon subcutaneously, effectively decrease the risk of hypoglycemia [6]. However, there is still a high risk of hyperglycemia in the case of an unannounced meal [7] due to the slow pharmacokinetics and pharmacodynamics of the SC route. The intraperitoneal (IP) route is the faster route for insulin and glucagon absorption compared to the SC route [8]. The IP-AP imitates pancreatic function by delivering insulin and glucagon to the peritoneal fluid and ultimately to the liver via the portal vein [9]. The fast insulin absorption in this route is proven efficient in BGL control without meal announcement [8].

Due to the novelty of using the IP route for treating diabetes and the lack of information, fewer studies have been done on the IP route compared to the SC route. However, the IP-AP has garnered interest due to recent developments in medical technology [1], [8], [10]; however, meal estimation is still needed to determine the appropriate insulin dosage even with the faster absorption of insulin from IP route.

Model predictive control (MPC) is a widely used control method in AP systems [11]. It requires a model, predictions, and estimates of GAR, as well as an estimation of immeasurable states to function effectively. Among the models proposed for the dual-hormone intraperitoneal artificial pancreas (DIP-AP) systems, our previously developed meta model [9] is accurate in predictions and offers the advantage of a simple and short identification process. Most meta model parameters were identified and validated through prior information from 26 animal experiments, and only four parameters require identification for each new subject.

The primary focus of this paper is the development of a complete-state moving horizon estimation (MHE) approach. This method utilizes statistical characteristics of GAR obtained

K. D. Benam, S. Gros, and A. L. Fougner are with the department of Engineering Cybernetics, Faculty of Information Technology and Electrical Engineering, Norwegian University of Science and Technology (NTNU), O. S. Bragstads Plass 2D, 7034 Trondheim, Norway. Email: {Karim.D.Benam, Sebastien.Gros, Anders.Fougner}@ntnu.no.

This research is funded by the Research Council of Norway (project no. 248872) and Centre for Digital Life Norway.

through the daily life of the patients to estimate the states and GAR. Moreover, we propose a technique to predict GAR without meal announcements to enable the MPC methods to predict BGL. To evaluate the effectiveness of our proposed estimator and predictor, we conducted animal experiments on three anesthetized pigs for a duration of 24 hours. While our primary objective in this study is to design an estimator for implementation in the MPC methods, it is important to recognize that the estimator can also be utilized in other control techniques, including PID or adaptive control methods. By incorporating the estimated and predicted GAR, these control methods can be better equipped to handle unannounced meals and exercise routines.

Our research group has previously presented a method based on MHE for detecting meals in single-hormonal subcutaneous AP systems in [12], and [13]. This approach showed promising results in simulations and was validated on clinical data. In addition, in a post-processing manner, a Kalman filter was designed to estimate the time and the size of the meal [14]. However, this method was not designed for real-time use. A different approach was investigated for early meal detection based on abdominal sound [15]. Similar studies have been conducted in IP AP systems using a Kalman filter [8] and a nonlinear high gain observer [16] based on the IP model presented in [17]. These methods use complex models with multiple states and require individual identification. This paper presents an estimator designed explicitly for control purposes in dual hormone IP AP systems. One novelty lies in using "meta model" particularly suited for MPC approaches [9], which significantly reduces the number of parameters to be identified, making the identification process more straightforward in closed-loop experiments. Another novelty is that the model includes both insulin and glucagon dynamics (both pharmacodynamics and pharmacokinetics), making the estimator suitable for a dual hormone system, while the other estimators reported in the literature were developed for single hormone systems.

The paper is structured as follows. Animal care and surgical procedures are described in Section II. Section III provides the models for DIP-AP and the intestines used in the estimator. The estimator is designed based on the animal model in Section IV. In Section V, a predictor scheme for closed-loop MPC techniques is suggested using the proposed models and the designed MHE. The demonstrative scenarios are employed in Section VI to examine the accuracy and reliability of the estimates and the predictions. The discussions and conclusions are provided in Sections VII and VIII, respectively.

II. Animal Experiments and Data

To evaluate the method proposed in this paper, we employed data from three animal experiments performed by our research group. This section provides a short overview of the experiments and the clinical procedures. The procedures are similar to the experiments described in [9], [18], [19].

A. Experiments and Animal Handling

There experiments were carried out on three, male non-diabetic farm pigs (Sus scrofa domesticus). The experiments were named "Experiment 1", "Experiment 2", and "Experiment 3," in this paper where the pigs weighed 36, 36, and 40 kg, respectively.

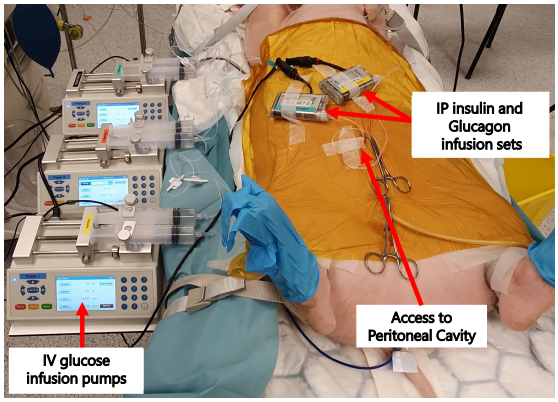

Fig. 1. The experimental setup of the dual-hormone intraperitoneal artificial pancreas for Experiment 1. The experiments were conducted on anesthetized pigs.

Before the experiments, the animals were given a week to adapt to the staff and their new environment. When possible, groups of animals were kept together. Before the experiment, they were provided unlimited access to water and twice-daily feedings of commercial growth feed. The procedure of inserting insulin and glucagon catheter into the peritoneal cavity, anesthesia, and euthanization at the end of the experiments is similar to the presented procedures in [9]. In order to suppress endogenous insulin and glucagon secretion, the pigs received octreotide as a 5µg/kg/h intravenous (IV) infusion. The experiments lasted up to 24 hours and the pigs were euthanized with an IV overdose of pentobarbital (100 mg/kg)(pentobarbital NAF, Apotek, Lørenskog, Norway) while fully anesthetized.

These experiments were carried out at the Norwegian University of Technology (NTNU) in accordance with "The Norwegian Regulation on Animal Experimentation" and "Directive 2010/63/EU on the protection of animals used for scientific purposes." Furthermore, the Norwegian Food Safety Authority (FOTS number 12948) approved the animal experiments.

B. Data

Each of the experiments lasted nearly 24 hours. In order to simulate a real-life scenario and mimic the intestine functions in anesthetized pigs, an IV glucose serum with a concentration of 200 mg/ml is used. The profile of the glucose infusion rate through the day is generated based on a human intestine model ("model 2") proposed in [20]. The scenarios are further discussed in Section IV-C.

Infusing the glucose intravenously to simulate the intestines in anesthetized pigs provides unique data to evaluate the performance of the estimator in detail. In order to infuse the glucose accurately according to the time, we used three programmable Chemyx Fusion 100 syringe pumps (Chemyx Inc., Stafford, TX, United States). The experimental setup in Experiment 1 is illustrated in Fig. 1. As shown in Fig. 1,

three glucose pumps were used in the experiments in parallel to avoid frequent refills of the syringe during the experiment.

Three Medtronic Enlite sensors (Northridge, CA, USA) with custom-made transmitters from Inreda Diabetic (Goor, the Netherlands) are used to measure the BGL during the experiment. The sensors are attached one day before the experiments. The Data acquisition system can connect to only two transmitters, and one of the sensors was a backup in case the two others failed. Of the two working sensors, the one with the most accurate performance was used in the controller. In order to choose the best sensor, blood samples were taken at varying sampling times between every 5–60 minutes and analyzed by an ABL800 FLEX analyzer (Copenhagen, Denmark). In these experiments, a dual hormone IP AP based on an MPC method was used to regulate the BGL within a normal range. This paper does not address the designed AP system; instead, only the data collected is used to evaluate the effectiveness of the proposed estimator, and the AP system will be reported elsewhere. The controller could give IP insulin or glucagon every 5 minutes using two infusion pumps provided by Inreda Diabetic (Goor, the Netherlands).

III. Background

A. Meta Model

The model used in this study is the meta model presented in [9]. Meta model (1) describes the interactions of BGL with IP insulin, IP glucagon, and IV glucose infusions.

$$\frac{d}{dt}\begin{pmatrix} \mathrm{x}_1 \\ \mathrm{x}_2 \\ \mathrm{x}_3 \\ \mathrm{x}_4 \\ \mathrm{x}_5 \\ \mathrm{x}_6 \\ \mathrm{x}_7 \end{pmatrix} = \begin{pmatrix} -\left(\beta_1+\beta_2\cdot \mathrm{x}_2+\beta_3\cdot \mathrm{x}_3\right)\cdot \mathrm{x}_1+HGP \\ \beta_5\left(-\mathrm{x}_2+\left(\beta_7\cdot\gamma_1\cdot \mathrm{x}_4-F_{sat}\right)\right) \\ \beta_8\left(-\mathrm{x}_3+F_{sat}\right) \\ -\gamma_1\cdot \mathrm{x}_4 \\ \beta_9\left(-\mathrm{x}_5+\beta_{10}\mathrm{x}_6\right) \\ -\gamma_2\cdot \mathrm{x}_6 \\ \gamma_3\cdot \mathrm{x}_3\cdot \mathrm{x}_1-\gamma_4\cdot HGP \end{pmatrix} + \begin{pmatrix} \gamma_7 G(t) \\ 0 \\ 0 \\ \gamma_8 I(t) \\ 0 \\ \gamma_9 H(t) \\ 0 \end{pmatrix} \tag{1}$$

In this model, $\{\mathrm{x}_1, \mathrm{x}_2, \mathrm{x}_3, \mathrm{x}_4\}$ are the states of the insulin sub-model including blood glucose level [mmol/l], effective insulin rate in the organs other than the liver [U/min], effective insulin rate in the liver [U/min], and concentration of insulin in the IP fluid [U/ml], respectively. In This sub-model, $I(t)$ is the IP insulin infusion rate [U/min], and $G(t)$ is the IV glucose infusion rate [mmol/min]. Notably, we assume that G is equivalent to the GAR in awake animals and represents the meal digestion rate in the intestines.

The term F_{sat} in this sub-model is used to model the saturation of the Hepatic first pass (HFP) effect, which is defined as follows:

$$F_{sat}(\mathrm{x}_4) \triangleq \beta_6 \frac{\beta_{13}\gamma_5 \mathrm{x}_4}{\beta_{12}+\beta_{13}\beta_7\gamma_1\mathrm{x}_4} \tag{2}$$

The states $\{\mathrm{x}_5, \mathrm{x}_6, \mathrm{x}_7\}$ are the states of the glucagon sub-model that includes effective glucagon rate in the liver [mg/min], glucagon concentration in the IP fluid [mg/ml], and glycogen storage level [%]. $H(t)$ is the IP glucagon infusion rate [mg/min], and HGP is the hepatic glucose production rate modeled as follows.

$$HGP \triangleq \beta_4 \mathrm{x}_5 \sqrt{\mathrm{x}_7}\cdot \exp\left(-\beta_{11}\cdot \mathrm{x}_3\right) \tag{3}$$

In (1), the parameter set $\{\beta_1, ..., \beta_4\}$ and the initial value of the glycogen storage level are needed to be identified individually. However, the parameters $\beta_5, ..., \beta_{13}$ are shown to be relatively fixed among the different pigs, and they are identified using the prior information of the other subjects. The parameters $\gamma_1, ..., \gamma_9$ are body-weight dependant parameters that are known functions (See equations (16) and (17) in [9]).

The equation (1) is discretized using the Euler method. Since 5 minutes is the most typical sample rate for CGM devices, that duration is chosen for the sampling time. The following equation represents the discretized system under the given assumptions.

$$x_{k+1} = F(x_k, G_k, I_k, H_k) + w_k \tag{4a}$$
$$y_k = Cx_k + v_k \tag{4b}$$

where the discretized right hand side of (1) is denotes as $F(x_k, G_k, I_k, H_k)$. y_k is the BGL and $C \triangleq [1\ 0\ 0\ 0\ 0\ 0\ 0]$. For the sake of simplicity, the discretized state vector $[\mathrm{x}_1, \mathrm{x}_2, \mathrm{x}_3, \mathrm{x}_4, \mathrm{x}_5, \mathrm{x}_6, \mathrm{x}_7]^T$ is denoted as x_k where the same notation applied for the inputs and measurements. w_k is the process noise, and v_k is the measurement noise.

B. Intestine Model

The model for the intestine used in this study to generate scenarios and design the predictor is "model 2" proposed in [20]. This model is given as follows.

$$\begin{cases} \dot{q}_{\text{sto1}} = -k_{21}\cdot q_{\text{sto1}} + D \\ \dot{q}_{\text{sto2}} = -k_{\text{empt}}\cdot q_{\text{sto2}} + k_{21}\cdot q_{\text{sto1}} \\ \dot{q}_{\text{gut}} = -k_{\text{abs}}\cdot q_{\text{gut}} + k_{\text{empt}}\cdot q_{\text{sto2}} \\ Ra(t) = f\cdot k_{\text{abs}}\cdot q_{\text{gut}} \end{cases} \tag{5}$$

where q_{sto1} and q_{sto2} are the weight of the solid and liquid glucose in the stomach, respectively. q_{gut} is the mass of the glucose present in the intestines. The size of the meal rate is D, and $Ra(t)$ is the glucose that appears in the blood via absorption in the intestines. The coefficient k_{empt} is the emptying rate of the stomach which is a nonlinear function defined as follows:

$$k_{\text{empt}}\left(q_{\text{sto}}\right) = k_{\min} + \frac{k_{\max}-k_{\min}}{2}\cdot\{\tanh\left[\alpha\left(q_{\text{sto}}-b\cdot D\right)\right] - \tanh\left[\beta\left(q_{\text{sto}}-c\cdot D\right)\right]+2\} \tag{6}$$

where $q_{\text{sto}} = q_{\text{sto1}} + q_{\text{sto2}}$. The other parameters of the model are positive constant values that are defined and given more in detail in [20].

Using the similar notation in the previous section and Euler approximation, one can find the discretized version of (5) in the following form:

$$q_{k+1} = F_q(q_k, D_k) + w_{q,k} \tag{7a}$$
$$Ra_k = C_q q_k + v_{q,k} \tag{7b}$$

where $F_q(.)$ is the discrete form of the right-hand side of the (5), $q_k \triangleq [q_{\text{sto1}}, q_{\text{sto2}}, q_{\text{gut}}]^T$, and $C_q \triangleq [0\ 0\ k_{\text{abs}}]$. Moreover, $w_{q,k}$ and $v_{q,k}$ are the process measurement noises, respectively.

C. Comments on the meta model and the CGM devices

In the design of the meta model, it is assumed that glucagon production in the pancreas is also affected in diabetes, and the pancreas is not able to produce glucagon. However, in the case of endogenous glucose production, G represents the meal digestion rate plus the endogenous glucose production (EGP) rate.

In the experiments, the BGL is measured using CGM devices. This system measures the concentration of glucose in interstitial fluid instead of the blood. The filters used in this CGM system and the process of glucose moving from blood to interstitial fluid cause a time lag in the measurements. In this paper, we ignored the measurement delays. However, the Kalman filter proposed in [21] can be used to compensate for the time lag. However, in this paper, we only used the sensor measurements for the sake of simplicity.

IV. Moving Horizon Estimation

In order to estimate the states of (4a), an approach similar to MHE is employed in this work. MHE is an optimization-based estimation technique for nonlinear systems where the current state of a system is estimated from a finite set of past measurements [22].

Regarding the accuracy of the different estimation techniques in nonlinear systems, MHE commonly outperforms standard state estimation approaches such as the extended Kalman filter (EKF). This is certainly relevant for nonlinear systems, which have been thoroughly considered in MHE. Unlike the EKF, MHE considers a horizon of recent measurements and a nonlinear model to estimate the state trajectories. In addition, using the MHE approach, one can estimate the sequence of the unknown inputs over the estimation horizon.

The capability and ease of accommodating constraints, prior knowledge of the states, or disturbances with non-Gaussian statistics are the other significant advantages of MHE. However, all of these advantages come at a higher computational cost. The basics of a standard MHE scheme are described in the following section.

A. Design of a Standard MHE with Assuming Glucose Appearance Rate is Known

The fundamental idea behind MHE is that the current state of the system is derived from a finite sequence of prior measurements taken within a time window of length N_{ob}. This sequence is subject to the disturbances and the model of the system.

The MHE can be expressed as an optimization problem in which the decision variables are the initial values of the states and the sequence of the process disturbances over the time estimation horizon. As an example, for the states (4a) and measurement (4b) with known G_k, I_k, and H_k, the MHE cost function takes the following form [23].

$$\Phi_1\left(\hat{x}_{t_0}, w_{t_0-1}, ..., w_{k-1}\right) = \Gamma_1(\rho) + \sum_{j=t_0}^{k} \mathcal{L}_1\left(w_{j-1}, v_j\right) \quad (8a)$$

subject to:

$$\rho = \hat{x}_{t_0} - \bar{x}_{t_0} \quad (8b)$$

$$\hat{x}_{k+1} = F(\hat{x}_k, G_k, I_k, H_k) + w_k \quad (8c)$$

$$v_k = y_k - C\hat{x}_k \quad (8d)$$

$$x_k \in \Omega_x, \quad w_k \in \Omega_w \quad (8e)$$

where $t_0 := K - N_{ob} + 1$, $\Gamma_1(\rho) := \rho^T P^{-1} \rho$ and $\mathcal{L}_1\left(w_k, v_k\right) := w_k^T Q^{-1} w_k + v_k^T R^{-1} v_k$. Matrices R and Q are covariance matrices of process noises and measurement noise, respectively. The term $\Gamma_1(\rho)$ is the arrival cost that carries prior information on the state of the system before time $k = t_0$. $\bar{x}_{t_0}$ is *a priori* state estimate and P represents the covariance of $\bar{x}_{t_0}$. Variable $\hat{x}_k$ is the estimated state vector at time k. Equation (8e) represents the constraints on the values of the states, process noises, and measurement noise, respectively.

The meals are not announced in the desired fully automated AP systems, and the GAR must be estimated. Similar to [12] and [13], one approach to estimate the GAR and detect the meals is to design and identify a model for the intestines (similar to equation (4) in [12]) to combine it with the meta model.

In the method mentioned above, the parameters of the intestine model need to be identified individually. Moreover, the glucose absorption rate is variable for the different types of meals. For example, the intestines absorb liquids faster than solid meals [20]. In addition, the EGP has different dynamics than the intestine. It is possible to employ a complex model for G to get around the problems mentioned above. However, it needs parameter identification, adds a higher computational cost, and requires additional information about the initial values and covariance matrices, which are not available.

In the next section, a dual-hormone intraperitoneal moving horizon estimator is designed to estimate the glucose appearance rate independently of the intestine model and based on measurements and prior knowledge about the lifestyle of the subjects.

B. Dual-hormone Intraperitoneal Moving Horizon Estimator with Unknown Glucose Appearance Rate

The main idea behind the estimator presented in this study is to directly estimate G over the MHE horizon based on the lifestyle of the patients. For the sake of simplicity, we recall the estimator in this section as Dual-hormone Intraperitoneal Moving Horizon Estimator (DIP-MHE).

We assumed that G is an input with a probability distribution function (PDF). An intestine and exercise model that generates the G based on the meals and the activities can be used to find the PDF function from the information gathered about the daily diets and exercise routines of the patients. The idea mentioned above can be formulated as followings:

$$\Phi_2\left(\hat{x}_{t_0}, \hat{G}_{t_0-1}, ..., \hat{G}_{k-1}, w_{t_0-1}, ..., w_{k-1}\right) = \Gamma_2(\rho) + \sum_{j=t_0}^{k} \mathcal{L}_2\left(w_{j-1}, v_j\right) + \sum_{j=t_0}^{k} \mathcal{J}\left(\hat{G}_j\right) \quad (9a)$$

subject to: (8b), (8d), (8e) and

$$\hat{x}_{k+1} = F(\hat{x}_k, \hat{G}_{g,k}, I_k, H_k) + w_k, \tag{9b}$$
$$\hat{G}_k \geq 0 \tag{9c}$$

in which $\Gamma_2(\rho) = \rho^T P_2^{-1} \rho$ and $\mathcal{L}_2(w_k, v_k) = w_k^T Q_2^{-1} w_k + v_k^T R_2^{-1} v_k$. where P_2, Q_2, and R_2 are positive definite matrices with the same definitions as in Section IV-A. The estimated glucose appearance rate is denoted as $\hat{G}_k$.

The term $\mathcal{J}(\cdot)$ is the prior knowledge embedded in the cost function to impose the feature of the G_k to the estimator. Therefore, $\mathcal{J}(\cdot)$ must be designed based on the body weight and the inverse distribution function (IDF) of G_k. One may use the $\log(\cdot)$ function or numerical approximation methods to obtain the IDF using the PDF.

We can use the statistics of G_k to embed the prior knowledge of GAR into the MHE. To achieve this, we must approximate the GAR according to the lifestyle and find its PDF. However, the complete information regarding the lifestyle and G might not be available, and the information that the approximate PDF provides for the MHE might be incomplete. We know that glucose absorption in the intestines and hepatic glucose production have slow dynamics and are continuous functions. Therefore, one can find the PDF of the $\Delta G_k := G_k - G_{k-1}$ (rate of GAR) as well and use it as an additional embedded prior knowledge for GAR.

Let us assume $f_r(G_k)$ and $f_{dr}(\Delta G_k)$ are PDFs of G_k and ΔG_k, respectively. In this case, one can use the following formulation to embed these PDFs in MHE by designing the $\mathcal{J}(\cdot)$ as follows:

$$\mathcal{J}(G_j) \triangleq p_r \cdot f_r^{-1}(G_j) + p_{dr} \cdot f_{dr}^{-1}(\Delta G_j) + p_{r_0}(G_j - \bar{G}_j)^2 \tag{10}$$

where $f_r^{-1}(G_j)$ and $f_{dr}^{-1}(\Delta G_j)$ are IDFs of G_j and ΔG_j, respectively. As mentioned earlier, the IDFs can be found using the $log(\cdot)$ function or numerically from the found PDFs. p_r and p_{dr} are positive constant scalars. In (10), $\bar{G}_j$ is the prior value chosen for the scalar G_j. Therefore, the term $p_{r_0}(G_j - \bar{G}_j)^2$ is similar to the arrival cost in the MHE. p_r, p_{dr}, and p_{r_0} are positive constant scalars.

The defined cost (10) embeds the approximated statistics of G_k to the estimator. The challenge in this approach is selecting $f_r(.)$ and $f_{dr}(.)$. These PDFs are time-varying, and they can change according to the changes in lifestyle and diet. For instance, the type and size of the meals can be chosen based on the body weight and diet to produce the G for the entire day, but if the patients change their diet, the type of food they eat, or the number of meals they eat throughout the day, the PDFs must be updated to reflect the new changes. We assumed that the patients followed a relatively consistent routine in their lifestyle regarding the number of meals per day, activity level, and the size of the meals relative to their body weight. Therefore, $f_r(.)$ and $f_{dr}(.)$ are considered as time-invariant functions. In the next section, a demonstrative example is provided to find $f_r(.)$ and $f_{dr}(.)$ for the animal experiments.

C. Probability Distribution Functions of Glucose Appearance Rate for a Demonstrative Scenario in Animal Experiment

As mentioned earlier, GAR must be found according to the lifestyle, diet, and physical characteristics of the patients. This section illustrates how to generate G and then find $f_r(.)$ and $f_{dr}(.)$ for the 24-hour anesthetized animal trial.

The IV glucose infusion is used in animal experiments to simulate the GAR. We simulated the EGP, main meals, and exercise events within 24 hours. The GAR is chosen to present significant challenges to the controller used in these experiments. The controller and experiment design are beyond the scope of this paper. The different elements of this scenario are defined as follows.

1) EGP Simulation: The basal rate of glucose production in adults is 2–8 mg/min/kg [24]. To prevent hypoglycemia and make sure that the pig received enough glucose during the experiment, we assumed that EGP has a constant rate during the day with a rate of 5 mg/min/kg.

2) Meal Simulation: To mimic the behavior of the intestines in the body and generate the GAR for a full-day experiment, we used the intestine (5) with the parameter identified in human trials listed in [20]. The experiments are scheduled to begin at 9:30 a.m. The times and sizes of meals are chosen based on body weight in the following manner:

- 11:00 a.m.: 0.30 gr/kg meal as a small breakfast.
- 01:00 p.m.: 0.70 gr/kg meal as a lunch.
- 06:45 p.m.: 1.00 gr/kg meal as a dinner.
- 09:45 p.m.: 0.60 gr/kg soft drink.
- 11:45 p.m.: 0.00 gr/kg sleeping.
- 03:50 a.m.: 0.70 gr/kg meal as a breakfast.

3) Exercise/Low Glucose Scenario: In reality, the impact of physical activity on BGL is multifaceted. Nonetheless, anesthetized animals cannot perform an exercise. Therefore, to *simulate* the effect of exercise at aerobic (low/medium) intensity, we lowered the glucose infusion from the baseline GAR. It was simulated as a "negative meal" (subtracted from the baseline glucose infusion) with a size of 0.25 mg/kg administered at 04:30 PM.

The designed scenario is illustrated in Fig. 2. Based on the designed scenario, we found the PDFs of G and ΔG_k. The gamma distribution function is chosen to define the probability feature of G since the glucose appearance rate is always a positive value. For the sake of simplicity, we assumed that G and ΔG_k are independent variables. In addition, it is assumed that ΔG_k has a normal distribution. With these assumptions, the estimated G over the MHE horizon can increase or decrease at the same rate due to the normal distribution of the ΔG_k independently of the estimated values for G.

In order to identify the parameters of the mentioned PDFs, the maximum likelihood method is used. The scenario for the experiments and the found PDFs are illustrated in Fig. 2.

D. Comments on the Designed DIP-MHE

In order to impose the prior knowledge to MHE, the cost (10) is proposed to embed into the standard MHE cost function. A Gamma PDF is identified for G. For simplicity, it is assumed that the ΔG_k has a normal distribution and is

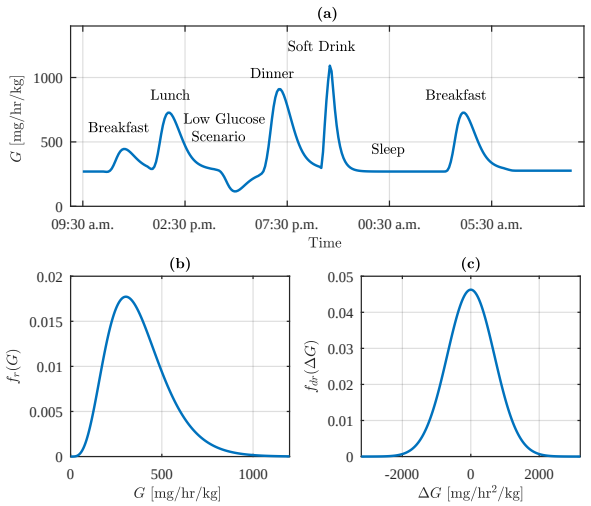

Fig. 2. The glucose appearance rate (G) designed for the 24-hour anesthetized animal experiments is shown in panel (a). The glucose was given intravenously. The fitted probability distribution functions of G (with gamma PDF) and ΔG_k (with normal PDF) are shown in panels (b) and (c), respectively.

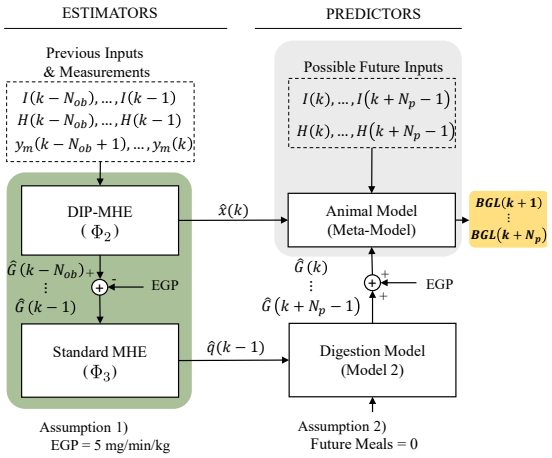

Fig. 3. The proposed BGL predictor scheme with unannounced meals. The estimators are shown in the green box. The problems Φ_2 and Φ_3 are solved sequentially to maintain modularity and simplicity of combining other observers instead of Φ_3. The gray box can be replaced with an MPC algorithm in the closed-loop system. BGL$(k+1)$, ..., BGL$(k+N_p)$ in the yellow box are the predicted blood glucose level.

independent of G_k. However, this simplification might not be accurate in real life, and the ΔG_k has a dependency on G_k. Additionally, the scenario is intended to last 24 hours due to the restrictions on the duration of the anesthetized animal trials. One should create weekly or monthly routines to achieve more accurate PDFs. Additionally, performing the exercise on anesthetized pigs is unfeasible. Thus, we have lowered the glucose infusion rate to simulate the impact of exercise at a low to medium aerobic intensity. Nonetheless, it is important to perform the actual exercise testing on awake animal subjects or proceed to the human phase for better evaluation of the designed estimator in exercise events.

V. Blood Glucose Predictor Scheme with Unannounced Meal

In the MPC methods, the BGL is predicted based on the possible combinations of future insulin and glucagon boluses. However, the future glucose appearance rates over the prediction horizon are needed to perform the predictions, while this information is unavailable when the meals are not unannounced. This section proposed an estimating scheme for short-term prediction of BGL that can be used for control purposes.

The idea is to estimate the states of the model 2 using the estimated GAR and predict it over the prediction horizon of N_p with assuming no meal over the time window $\{k, ..., k+N_p-1\}$. Different methods, such as EKF, high-gain observers, and others, can also be used to estimate the states of the digestive model at each sampling time with $\hat{G}$ (the estimated GAR using the DIP-MHE). However, a standard MHE approach is used in this paper with the following cost function to estimate the states of the intestine model (7a) – (7b).

$$\Phi_3\left(\hat{q}_{t_0}, w_{q,t_0-1}, w_{q,t_0}, ..., w_{q,k-1}\right) = \Gamma_3(\rho_q) + \sum_{j=t_0}^{k} \mathcal{L}_3\left(w_{q,j-1}, v_{q,j}\right) \quad (11a)$$

subject to:

$$\rho_q = \hat{q}_{t_0} - \bar{q}_{t_0} \quad (11b)$$

$$\hat{q}_{k+1} = F_q(\hat{q}_k, \hat{G}_k) + w_{q,k} \quad (11c)$$

$$v_{q,k} = (\hat{G}_k - \text{EGP}) - C_q \hat{q}_k \quad (11d)$$

$$q_k \in \Omega_q, \quad w_{q,k} \in \Omega_{w,q}, \quad v_{q,k} \in \Omega_{v,q} \quad (11e)$$

in which $\Gamma_3(\rho_q) = \rho_q^T P_q^{-1} \rho_q$ and $\mathcal{L}_3\left(w_{q_j}, v_{q_j}\right) = w_{q_j}^T Q_q^{-1} w_{q_j} + v_{q_j}^T R_q^{-1} v_{q_j}$. Notably, the positive definite matrices P_q, Q_q, and R_q have the same definition as P, Q, and R in (8a), respectively. The output of model 2 (7a) – (7b) is the glucose absorbed from the intestines and does not consider the EGP. Therefore, one must deduct the EGP from $\hat{G}$ as in (11d). For the predictions, we must add the EGP to the predicted glucose absorbed from the intestines to obtain the total predicted GAR.

The proposed block diagram for the predictor is shown in Fig. 3, with having the estimates of the model 2 at time $k-1$ and assuming no meal consumption in the prediction horizon with the length of N_p, one can have an estimation of G for the future time samples of $\{k, k+1, ..., k+N_p-1\}$. Having the $\hat{x}_k$ together with predicted G enables us to predict the BGLs for any future insulin and glucagon boluses using the meta model.

A. Comments on the Designed Predictor

The predictor assumes that no meals will be consumed during the prediction period, which could lead to an underestimation of BGL if a meal will be consumed. However, underes-

timating meals could prevent excessive insulin administration and reduce the risk of postprandial hypoglycemia.

A limitation of the proposed scheme is the increased computational cost associated with solving Φ_2 and Φ_3 separately. However, the problems Φ_2 and Φ_3 could be combined, but this would lead to undesirable interactions between the parameters of the model 2 and the estimation of the states of the meta model and G_k. Solving the problems Φ_2 and Φ_3 in a sequence is made for ease of tuning the estimators, reducing complexity, and maintaining the modularity of the method.

VI. Demonstrative Examples

The performance of the DIP-MHE and the proposed predictor scheme is evaluated using the test data from three animal experiments in this section. To this aim, two scenarios are designed; Scenario 1 evaluates the performance of the DIP-MHE in a post-processing manner, and Scenario 2 evaluates the performance of the proposed predictor scheme for closed-loop systems. These scenarios are described in the following sections.

A. Scenario 1, Performance Evaluation of the DIP-MHE in Post-Processing:

This scenario evaluates the performance of the designed DIP-MHE in estimating the glucose appearance rate, states, robustness of the estimator to model mismatches, and the reliability of the estimates. Three sub-scenarios have been created to simulate real-world situations and test the performance of the proposed method in detail:

1) Scenario 1.A, Accuracy of Glucose Appearance Rate Estimates: This scenario aims to evaluate the performance of the DIP-MHE in estimating the GAR. As shown in Fig. 4, the estimated GAR is compared with the rate of the infused IV glucose during the experiments. In this scenario, the parameters of the meta model are identified individually. However, in closed-loop tests and experiments on awake animals, the available data for identification is limited, which could impact the accuracy of the meta model and subsequently and the performance of the estimator. These cases are discussed later in Scenarios 1.C and 2.

2) Scenario 1.B, Accuracy of the State Estimates: This scenario focuses on evaluating the ability of the DIP-MHE to estimate the states of the meta model. The estimated states must be compared to their actual values to assess the performance accurately. However, the states $\mathrm{x}_2, \mathrm{x}_3, \mathrm{x}_4, \mathrm{x}_5, \mathrm{x}_6, \mathrm{x}_7$ are not directly measurable. We assumed that the time lag of the CGM sensors is negligible, the only measurable quantity in these experiments is x_1, which is obtained using CGM systems.

As previously mentioned, the primary goal of the DIP-MHE is to enable accurate predictions for use in MPC techniques. Therefore, the performance of the DIP-MHE in estimating $\hat{x}_k$ can be indirectly evaluated by comparing the predicted BGL with the measured BGL in a post-processing manner, assuming that the future glucose infusion is known to the model. As shown in Fig. 3, the predicted BGL is obtained by using the estimated $\hat{x}_k$, feature inputs, and the identified meta model.

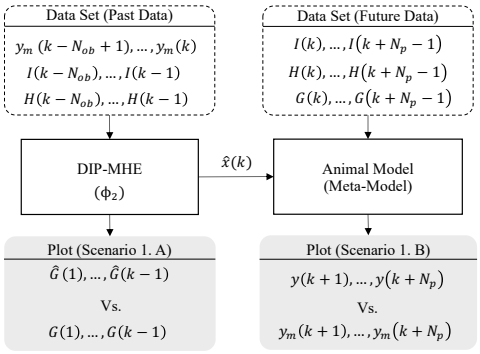

Fig. 4. Scenario 1.A and Scenario 1.B are illustrated. In Scenario 1.A, the performance of DIP-MHE in estimating glucose infusion rate (GAR) is evaluated by comparing it to the actual rate of intravenous glucose infusion during the experiments. In Scenario 1.B, the performance of DIP-MHE in estimating the states is evaluated indirectly by comparing the predicted blood glucose level (BGL) based on an animal model to the measured BGL in a post-processing manner. N_{ob} and N_p represent the estimation and prediction horizons, respectively.

The predicted BGL is then compared with the measured BGL. This comparison is considered as an indirect evaluation of the DIP-MHE in estimating $\hat{x}_k$. To ensure that the evaluation is accurate, the selected prediction horizon (N_p) must be long enough to cover a full meal; in this scenario, $N_p = 48$ samples, or 4 hours, were chosen.

The initial value selected for the states are $\hat{x}_0^T = [y_{m0}, 0, 0, 0, 0, 0, 30]$ where y_{m0} is the first BGL measured at time $k = 1$. In addition, the initial glucose appearance rate is set to $G_j = 5$ mg/min/kg for $j = [1, N_{ob} - 1]$, which is equal to the basal body glucose appearance rate [24]. Regarding the initial values chosen ($\hat{x}_0^T$), it is known that there has been no presence of insulin or glucagon in the bloodstream or peritoneal fluid for an extended period of time. However, the selected glycogen storage level is based on previous subjects and there is less confidence in the chosen initial glycogen value for each new subject. Additionally, the accuracy of selecting $Gj = 5$ mg/min/kg for $j = [1, Nob - 1]$ is uncertain. To address these uncertainties, a warm-up period was considered for the designed estimator using initial samples of the experiment. During the warm-up period, the arrival cost was set to ${P_3}^{-1} = \mathrm{diag}(25, 25, 25, 100, 5, 5, 10^{-3})$. The warm-up period was set to 180 minutes (36 samples), which is longer than the half-life time of IP insulin, glucagon, and the tail of the glucose absorption due to the meal. After the warm-up period, the arrival cost coefficient will increase to ${P_3}^{-1} = 100 \times \mathrm{diag}(50, 50, 50, 100, 50, 50, 0.5)$.

The matrix ${R_3}^{-1}$ is the inverse of covariance of the measurement noise, and generally speaking, it is a scaling penalty on how accurately the model output ($\hat{y}_k$) must be fitted to the measurements (y_{mk}) over the time estimator horizon. In this paper, this matrix is chosen as ${R_3}^{-1} = 10^2 \times \mathbb{I}$ where $\mathbb{I}$ is a $N_{ob} \times N_{ob}$ identity matrix. Other tuning parameters are $p_r = 1$, $p_{dr} = 1$, $p_{r_0} = 1$, and $Q_3 = 0_{7\times7}$. For simplicity, we considered that there is no process noise or endogenous insulin and glucagon production. The parameters are tuned to achieve satisfactory results for the first experiments and then tested on the other experiments.

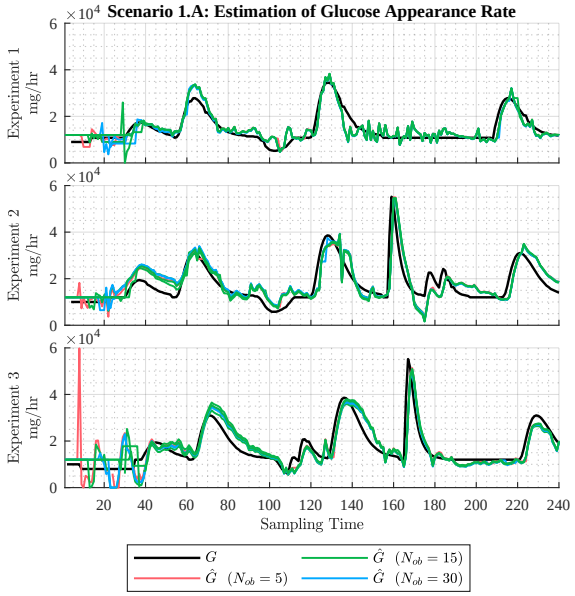

Fig. 5. The figure illustrates the performance of the proposed DIP-MHE in Scenario 1.A, by comparing the glucose appearance rate (G) given to the pigs via the IV route to the estimations ($\hat{G}$) made by DIP-MHE for different observation horizons (N_{ob}).

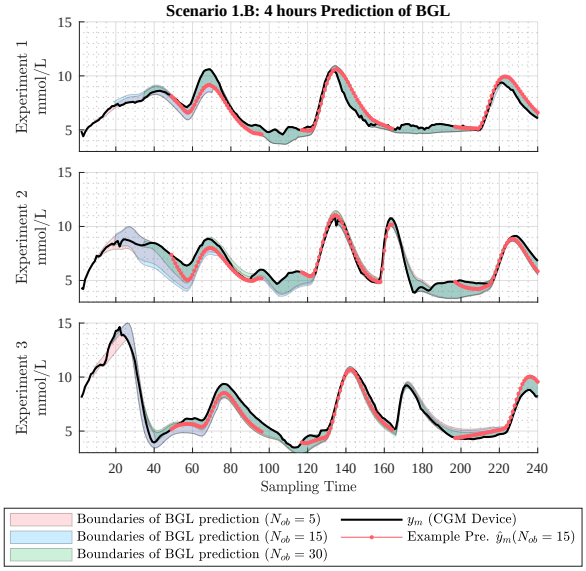

Fig. 6. The figure illustrates the performance of the proposed DIP-MHE in Scenario 1.B by comparing the four-hour BGL predictions (based on estimated GAR and the states) to the measured BGL using the CGM (y_m). The predictions are made at every sampling time, and the shaded area shows the boundaries of predicted BGL at each sampling time. As an example, the predicted trajectories are shown for each meal for an observation horizon of $N_{ob} = 15$.

It is important to note that the population parameters of model (1) are identified based on short-term anesthetized pig experiments and as it is mentioned in [9], the charging rate of glycogen (γ_3) is identified near zero. We found a better performance of the estimator when replacing γ_3 with $0.8\beta_3$. From a philological point of view, it means that the 80% of the up-taken glucose in the liver will be saved as accessible glycogen.

A key parameter in the DIP-MHE design is N_{ob}, which can impact the estimation accuracy, convergence, and computational complexity. From an accuracy standpoint, longer estimation horizons are preferable as the estimator will have access to more information about the dynamics of the system from measurements. However, using longer horizons can increase computational difficulty.

TABLE I
MEAN ABSOLUTE PERCENTAGE ERROR (MAPE) OF THE PROPOSED DIP-MHE IN ESTIMATING THE GLUCOSE APPEARANCE RATE (G) AND THE MAPE OF THE FOUR-HOUR BGL PREDICTION (AVERAGED OVER ALL SAMPLING TIMES) IN SCENARIO 1.A AND SCENARIO 1.B, RESPECTIVELY.

	MAPE (G) [%]				MAPE (BGL Pre.) [%]			
N_{ob}	Exp 1	Exp 2	Exp 3	**Ave.**	Exp 1	Exp 2	Exp 3	**Ave.**
5	16.9	23.9	24.1	**21.6**	8.3	12.0	9.5	**9.9**
10	16.6	26.3	23.0	**22.0**	8.9	12.4	8.3	**9.9**
15	17.2	26.5	23.1	**22.3**	9.0	12.2	9.0	**10.1**
20	17.0	26.0	23.1	**22.0**	8.9	12.0	9.0	**10.0**
25	17.8	24.7	24.2	**22.2**	9.1	11.5	9.7	**10.1**
30	17.0	23.7	20.6	**20.4**	9.3	11.3	9.0	**9.9**
Ave.	17.1	25.2	23.0	**21.8**	8.9	11.9	9.1	**10.0**

In order to find the suitable horizon length, performance analysis is done for $N_{ob} = \{5, 10, ..., 30\}$. The sampling time is 5 minutes and, therefore, $N_{ob} \times dt = \{25, 50, ..., 150\}$ minutes. We found that the half-life of the IP insulin and glucagon in the pigs is less than 100 minutes [25]. Therefore, the maximum estimation horizon evaluated in this paper is set at 150 minutes.

For the selected set of N_{ob}, the mean absolute percentage error (MAPE) of estimating glucose appearance rate and the MAPE of the four-hour predictions are shown in Table I. As an example, for $N_{ob} = \{5, 15, 30\}$ the estimated G_k and the boundaries of the four-hour predicted BGL are illustrated in Fig. 5 and Fig. 6, respectively. In experiment 1, we did not carry out the simulation of the soft drink as the heart rate was elevated following dinner. Once the heart rate returned to normal, we proceeded with simulating sleep.

A similar performance is achieved for all three experiments with a fixed tuning of DIP-MHE and different values of N_{ob}. The DIP-MHE has achieved an average MAPE of 21.8% in estimating GAR (Scenario 1.A) and an average MAPE of 10% in predicting the BGL for four hours (Scenario 1.B).

In the third experiment (as shown in Fig. 6), the insulin and glucagon pumps were intentionally misconnected (their reservoirs interchanged) as a simulation of user error. This resulted in elevated glucose levels at the start of the experiment. We believe that this simulated user error also affected the response of the pig to insulin later in the experiment, as the animal did not receive insulin for an extended period of time.

As shown in Fig. 7, when the number of observations, N_{ob}, is high, the ability to predict BGL is greatest during the transient period. This suggests that the accuracy of state estimation improves as the estimation horizon is extended. However, this improvement comes at the cost of longer computation times. On a regular desktop PC, the average computation time for $N_{ob} = 5, 10, ..., 30$ are 2.33, 2.87, 2.90, 3.14, 3.37, and 3.95 seconds, respectively. However, due to

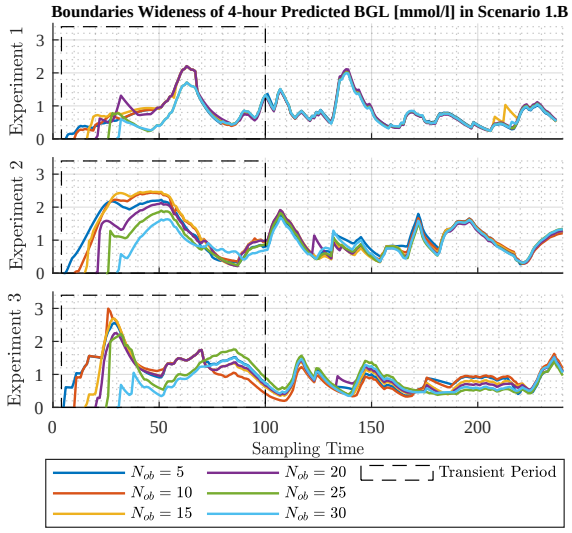

Fig. 7. The wideness of the boundaries of the predicted BGL in Scenario 1.B refers to how much variation there is in the predicted values. It can be an indication of how uncertain or confident the prediction is. It is important to have less wide boundaries when it comes to predicted BGL, which is necessary for managing diabetes.

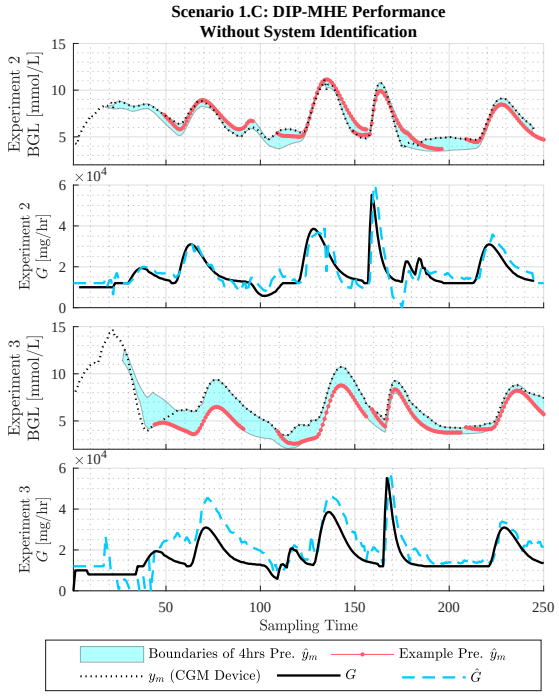

Fig. 8. The figures show the estimated glucose appearance rate and the boundaries of the BGL prediction in Scenario 1.C. Estimations are done with $N_{ob} = 15$. The predictions and the estimations are made using the identified meta model [9] for experiment 1. y_m is the measured BGL using the CGM device, G is the given IV glucose infusion during the experiments, and $\hat{G}$ is the estimated GAR.

the large sampling intervals (5 minutes), the calculations are done without optimizing the simulation codes.

3) Scenario 1.C, Performance of the DIP-MHE with model mismatches:

In the previous scenarios, a satisfactory performance in estimating the glucose appearance rate and prediction of the BGL is achieved using the proposed DIP-MHE. This is done using the tuned DIP-MHE on the first experiment and the model, identified individually using their full-day BGL measurements. In the short-term closed-loop animal experiments, there are not enough BGL measurements to identify the individual parameters of the meta model ($\{\beta_1, \beta_2, \beta_3, \beta_4\}$). In addition, tuning the parameters of the DIP-MHE is challenging to perform during the experiments.

A practical way to address these challenges is to leverage information from previous experiments, such as utilizing data from a pig with a similar body weight, to tune the parameters of the meta model and DIP-MHE for new experiments. We refer to this data from prior experiments as "training data". This approach can help overcome the challenges and ensure accurate estimations. However, the insulin and glucagon responses differ from pig to pig. Therefore, the performance of the DIP-MHE in the presence of the model identification error must be studied. To that end, we proposed Scenario1.C, in which the first experiment serves as training data and the DIP-MHE is then performed on the second and third experiments without re-tuning and model identification.

Fig. 8 and Table II provide details on the performance of the DIP-MHE in Scenario 1.C. The DIP-MHE had the same settings as Scenario 1.A, with $N_{ob} = 15$.

The estimator was able to achieve an accurate estimation of the GAR for experiment 2, with a MAPE of 23.3%. Furthermore, it was able to generate a four-hour blood glucose level (BGL) prediction with an average MAPE of 12.9%. For the third experiment, there is a bias and error in estimating the glucose appearance rate in the first 100 samples. As explained earlier, this is due to the simulated user error in the third experiment. The MAPE of GAR estimation and BGL prediction decreased to 28.3% and 17.1%, respectively, for the rest of the experiment.

TABLE II
MEAN ABSOLUTE PERCENTAGE ERROR (MAPE) OF THE PROPOSED DIP-MHE IN ESTIMATING THE GLUCOSE APPEARANCE RATE (G) AND THE MAPE OF THE FOUR-HOUR BGL PREDICTION (AVERAGED OVER ALL SAMPLING TIMES) IN SCENARIO 1.C.

MAPE (G) [%]				MAPE (BGL Pre.) [%]			
Exp 2	Exp 3	Exp 3$^{(1)}$ (Part 1)	Exp 3$^{(2)}$ (Part 2)	Exp 2	Exp 3	Exp 3$^{(1)}$ (Part 1)	Exp 3$^{(2)}$ (Part 2)
23.3	41.3	61.3	28.3	12.9	20.2	27.5	17.1

(1) Part 1: $[0, 500]$min. (Effect of the user error simulation).
(2) Part 1: $[505, 1265]$min.

B. Comments on the Reliability of the Estimates

The proposed DIP-MHE has been shown to accurately estimate GAR and predict BGL in a post-processing manner. However, when using the estimator in closed-loop systems, it is essential to consider the reliability of the estimator. Various methods have been proposed in the literature for analyzing the stability of the MHE, such as the approaches in [26]. One way to analyze the estimator is by finding the covariance of the estimates, which can be challenging. However, the inverse of the Hessian matrix can be used as an approximation for the

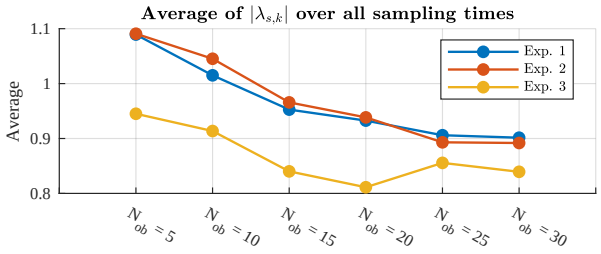

Fig. 9. Average of $|\lambda_{s,k}|$ over all for different N_{ob} and experiments.

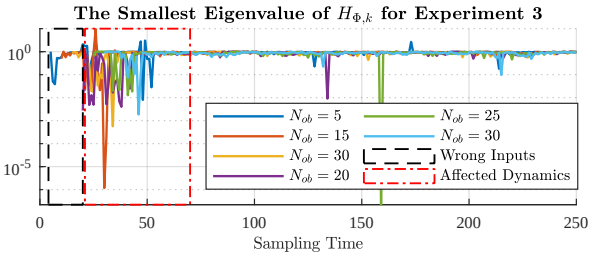

Fig. 10. The smallest eigenvalues of the $H_\Phi(k)$ of the experiment 3 plotted for different N_{ob}. The black box shows the period where glucagon boluses were given instead of insulin, and the pig did not receive insulin. The red box indicated the period that the authors believe that the metabolic dynamics have been affected due to the prolonged lack of insulin at the beginning of the experiment.

covariance matrix of estimation error, as shown by Gejadze *et al.* in [27]. The Hessian matrix is defined as:

$$H_{\Phi,k} := \nabla^2 \Phi_{2,k} \tag{12}$$

Where $\Phi_{2,k}$ is the cost function (9a) minimized at the sampling time k. $H_{\Phi,k}$ is the Hessian matrix found for the estimates at time k.

The fact mentioned above has been a well-known finding in statistics for decades, and multiple studies offer the same conclusion. Nevertheless, there has also been considerable ambiguity which has been discussed in [27].

As mentioned earlier, the matrix $H_{\Phi,k}$ must be calculated at each sample time after the estimations are complete. The constraints mentioned in (8e) and (9c) are positive constraints, meaning that the states and G are zero or greater than zero. We assume that the covariances of the active constraints (parameters estimated as zero) are actually zero. For example, the amount of glucagon in the peritoneal cavity (x_6) is zero before or after glucagon boluses since there is no glucagon infusion into the cavity except by pumps. Therefore, the rows and columns of $H_{\Phi,k}$ corresponding to the active constraints will be removed. To prevent numerical errors in finding the inverse of $H_{\Phi,k}$, we calculate $\lambda_{s,k}$, which is the smallest eigenvalue of $H_{\Phi,k}$ and defined as follows.

$$\lambda_{s,k} := \min \ \{\det(H_{\Phi,k})\} \tag{13}$$

The estimates corresponding to $\lambda_{s,k} \rightarrow 0$ have large covariance, which indicates less reliable estimates.

Fig. 9 illustrates the average absolute values of $\lambda_{s,k}$ for all sampling times in all experiments. The trend in this graph shows that longer horizon length results in 10-18% lower values for $\lambda_{s,k}$, which means the average reliability of the estimates decreases with large values for N_{ob}.

The reliability of the estimates for experiments 1 and 2 are similar even though the parameters of their models are different. Experiment 2 had a different glucose infusion profile due to the soft drink consumption. However, DIP-MHE showed less reliable estimates than the third experiment due to the simulated user error at the beginning of the experiment.

The authors believe that the lack of insulin in the blood for a long period of time and a high BGL may affect the dynamics of the metabolic system. $\lambda_{s,k}$ for the third experiment is shown in Fig. 10. The eigenvalues for the time interval $k \in [20, 50]$ (the period after simulated user error) are smaller than the rest of the experiment for all $N_{ob} = \{5, 10, 15, 20, 25, 30\}$. It is also evident from Fig. 5 and Fig. 6 that the estimates of DIP-MHE are unreliable for this period. The absence of insulin boluses (no exciting inputs) and the prolonged lack of insulin in the bloodstream can contribute to the small $\lambda_{s,k}$ at $k \in [20, 50]$ and practical unidentifiablity in experiment 3. This is a good indication that the inverse Hessian matrix can serve as an approximation of the covariance matrix and the reliability metric in closed-loop applications.

C. Scenario 2, Prediction Performance in Closed-loop System:

This scenario uses the tuned DIP-MHE in Scenario 1.C to evaluate the proposed predictor method in Section V. This scenario aims to evaluate the performance of the proposed prediction scheme in MPC methods. The main difference from Scenarios 1.C, is that in Scenario 2 the future GAR is unknown and is instead predicted. At each sampling time, the future insulin and glucagon infusions are assumed to be known, since we want to compare the predicted BGL trajectories with the actual measured BGL in the experiments. In closed-loop systems, the MPC provides the future insulin and glucagon.

In order to tune the cost function (11a), the measurements of Experiment 1 are used as training data. In this tuning, the estimated glucose appearance rate covariance is considered constant and $R_q = 10^{-2} \times \mathbb{I}$ where $\mathbb{I}$ is a $N_{ob} \times N_{ob}$ identity matrix. The other tuning parameters are chosen as $Q_q^{-1} = \text{diag}(0.01, 0.01, 1)$, $P_q^{-1} = \text{diag}(0.01, 0.01, 0.01)$, and $N_{ob} = 15$.

In a closed-loop experiment, the prediction horizon must be chosen based on the dynamics of the system, available computing power, uncertainties, and disturbances. The main effect (half-life) of IP insulin and IP glucagon is seen within the first 100 minutes (20 samples) after injection; therefore, a prediction horizon of 120 minutes is sufficiently long for the model-based predictive controllers. Additionally, predicting the GAR for a longer horizon can be extremely uncertain because of unannounced meals.

The predicted trajectories of the BGL and the GAR are illustrated in Fig. 11. As shown in Table III, the proposed method could predict the BGL and GAR with an average MAPE of 18.1% and 28.4%, respectively.

As previously stated, the glucose appearance rate is estimated passively from the revolutions in the BGL since the

Fig. 11. Performance of the proposed DIP-MHE and the predictor scheme in Scenario 2 for the three animal experiments; In this scenario, the BGL and glucose appearance rate predictions are made using the scheme proposed in Fig. 3. The parameters of the meta model (1), the estimators (9a), and (11a) are identified and tuned using the first experiment. y_m is the measured BGL via the CGM Device, and $\bar{y}_m$ is the predicted BGL. G is the IV glucose infusion rate during the experiments, $\hat{G}$ is the estimated glucose infusion rate by DIP-MHE, and $\bar{G}$ is the predicted glucose infusion rate made for 120 minutes without any meal announcement.

TABLE III
MEAN ABSOLUTE PERCENTAGE ERROR (MAPE) OF THE PROPOSED METHOD IN PREDICTING THE GLUCOSE APPEARANCE RATE (G PRE.) AND THE MAPE OF BGL PREDICTION (BGL PRE.) FOR 120 MINUTES IN SCENARIO 2.

	MAPE (G Pre.) [%]				MAPE (BGL Pre.) [%]			
N_{ob}	Exp 1	Exp 2	Exp 3	**Ave.**	Exp 1	Exp 2	Exp 3	**Ave.**
15	12.7	19.7	22.0	**18.1**	23.6	31.4	30.2	**28.4**

meal amount, meal time, and type of meals are not predictable without the meal announcement. Furthermore, eating is a continuous process; the amount of glucose given to the stomach and intestinal system continuously rises. Therefore, the predicted BGL diverge from the actual future BGL just before the meal absorption starts and during the meal, as seen in Fig. 11. However, as more BGL measurements are obtained, the predictions are updated and become more precise.

The proposed scenario for the second and third experiments is the worst-case scenario. The DIP-MHE and the model have been tuned and identified using data from the first experiment. In real-world situations, such as human trials or longer animal experiments, there would be sufficient data to identify the model and tune the DIP-MHE individually.

In summary, the proposed predictor based on the DIP-MHE performed reasonably well in experiments 2 and 3. The predictions of the GAR over shots during the fast glucose rise (the soft-drink event) in the second experiment. It is important to consider the overshoots of the proposed prediction scheme when designing an MPC controller.

VII. DISCUSSION

This study focuses on designing an estimator and predictor for the GAR and meta model states, which can be applied in MPC methods. The meta model is based on animal data using intraperitoneal injection of insulin and glucagon. To utilize this method in human trials, the model needs to be adapted to human data. Although designed for dual-hormone systems, the method can also be used in insulin-only APs. However, the use of the intraperitoneal route has some challenges, which are discussed in [8]. Alternatively, the proposed method can also be used in currently available insulin-only APs using subcutaneous injections. To this end, the IP model used in the estimator needs to be substituted with an SC model that provides comparable accuracy. However, this replacement necessitates the recalibration and optimization of the parameters. Specifically, due to the slower dynamics of the SC route, it may be necessary to select a longer estimator horizon

for improved performance. Although the intraperitoneal route is more invasive and costly, it has the advantage of faster insulin absorption, which makes it easier to avoid oscillations and thereby achieve larger safety margins and achieve a lower average glucose level. We utilized data from three comprehensive experiments in anesthetized animals. However, further experiments with longer duration are required before implementing the method in humans.

VIII. Conclusions

The proposed DIP-MHE is tested in animal experiments in near-real-life conditions and with model mismatches. It is shown to be a reliable and effective method for estimating the glucose appearance rate and states of the metabolic system. The proposed predictor scheme can be used in closed-loop systems to make accurate predictions of the BGL, allowing for more precise insulin and glucagon bolus calculations without human interventions. Furthermore, the estimator can be utilized to estimate glucose absorption from the intestines to develop and identify an accurate model for the digestive system. The method has been successfully tested in animal trials and has the potential to be adapted for use in human trials.

IX. Acknowledgments

The animal experiments were performed at the Comparative Medicine Core Facility (CoMed) at the Norwegian University of Science and Technology (NTNU). The study was supported by the Norwegian Research Council (under project number 248872) and the Centre for Digital Life Norway. In addition, the CGM systems and the infusion pumps are provided by Inreda Diabetic company (Goor, the Netherlands) for the experiments at no cost. The experiments outlined in this paper were conducted by Marte Kierulf Åm, Patrick Christian Bösch, Hasti Khoshamadi, Oddveig Lyng, and Karim Davari Benam. The authors would like to thank this team for their invaluable contribution to performing the experiments and collecting the data. We also like to thank Professor Sven Magnus Carlsen for his help in designing the experiments and discussions. This study was conducted as part of the efforts of the Artificial Pancreas Trondheim research group (APT, apt-norway.com) to develop a fully automated artificial pancreas.

References

[1] C. Cobelli et al., "Artificial pancreas: past, present, future," *Diabetes*, vol. 60, no. 11, pp. 2672–2682, 2011.

[2] A. El Fathi et al., "A model-based insulin dose optimization algorithm for people with type 1 diabetes on multiple daily injections therapy," *IEEE Transactions on Biomedical Engineering*, vol. 68, no. 4, pp. 1208–1219, 2020.

[3] J. Langholz et al., "Fully automated bi-hormonal intraperitoneal artificial pancreas using a two-layer pid control scheme," in *2023 European Control Conference (ECC)*. IEEE, 2023, pp. 1–8.

[4] A. Haidar, "The artificial pancreas: How closed-loop control is revolutionizing diabetes," *IEEE Control Systems Magazine*, vol. 36, no. 5, pp. 28–47, 2016.

[5] A. Brazeau et al., "Carbohydrate counting accuracy and blood glucose variability in adults with type 1 diabetes," *Diabetes research and clinical practice*, vol. 99, no. 1, pp. 19–23, 2013.

[6] T. Peters and A. Haidar, "Dual-hormone artificial pancreas: benefits and limitations compared with single-hormone systems," *Diabetic Medicine*, vol. 35, no. 4, pp. 450–459, 2018.

[7] E. Fushimi et al., "A dual-hormone multicontroller for artificial pancreas systems," *IEEE Journal of Biomedical and Health Informatics*, vol. 26, no. 9, pp. 4743–4750, 2022.

[8] C. Toffanin et al., "Artificial pancreas: In silico study shows no need of meal announcement and improved time in range of glucose with intraperitoneal vs. subcutaneous insulin delivery," *IEEE Transactions on Medical Robotics and Bionics*, vol. 3, no. 2, pp. 306–314, 2021.

[9] K. D. Benam et al., "Identifiable prediction animal model for the bi-hormonal intraperitoneal artificial pancreas," *Journal of Process Control*, vol. 121, pp. 13–29, 2023.

[10] J. Lo Presti et al., "Intraperitoneal insulin delivery: evidence of a physiological route for artificial pancreas from compartmental modeling," *Journal of diabetes science and technology*, p. 19322968221076559, 2022.

[11] D. Shi et al., "Adaptive zone model predictive control of artificial pancreas based on glucose-and velocity-dependent control penalties," *IEEE Transactions on Biomedical Engineering*, vol. 66, no. 4, pp. 1045–1054, 2018.

[12] K. Kölle et al., "Meal detection based on non-individualized moving horizon estimation and classification," in *2017 IEEE Conference on Control Technology and Applications (CCTA)*. IEEE, 2017, pp. 529–535.

[13] K. Kölle et al., "Pattern recognition reveals characteristic postprandial glucose changes: Non-individualized meal detection in diabetes mellitus type 1," *IEEE journal of biomedical and health informatics*, vol. 24, no. 2, pp. 594–602, 2019.

[14] O. M. Staal et al., "Meal estimation from continuous glucose monitor data using kalman filtering and hypothesis testing," in *2019 IEEE 58th Conference on Decision and Control (CDC)*. IEEE, 2019, pp. 5654–5661.

[15] K. Kölle et al., "Feasibility of early meal detection based on abdominal sound," *IEEE Journal of Translational Engineering in Health and Medicine*, vol. 7, pp. 1–12, 2019.

[16] K. D. Benam et al., "Full order high gain observer design for image-guided robotic flexible needle steering," in *2019 27th Iranian Conference on Electrical Engineering (ICEE)*. IEEE, 2019, pp. 1151–1156.

[17] C. Lopez-Zazueta et al., "Low-order nonlinear animal model of glucose dynamics for a bihormonal intraperitoneal artificial pancreas," *IEEE Transactions on Biomedical Engineering*, 2021.

[18] I. Dirnena-Fusini et al., "Intraperitoneal insulin administration in pigs: effect on circulating insulin and glucose levels," *BMJ Open Diabetes Research and Care*, vol. 9, no. 1, p. e001929, 2021.

[19] M. K. Åm et al., "Intraperitoneal and subcutaneous glucagon delivery in anaesthetized pigs: effects on circulating glucagon and glucose levels," *Scientific reports*, vol. 10, no. 1, pp. 1–8, 2020.

[20] C. Dalla Man et al., "A system model of oral glucose absorption: validation on gold standard data," *IEEE Transactions on Biomedical Engineering*, vol. 53, no. 12, pp. 2472–2478, 2006.

[21] M. Halvorsen et al., "Blood glucose level prediction using subcutaneous sensors for in vivo study: Compensation for measurement method slow dynamics using kalman filter approach," in *2022 IEEE 61st Conference on Decision and Control (CDC)*, 2022, pp. 6034–6039.

[22] J. Kang et al., "A simultaneous parameter and state estimator for polymerization process based on molecular weight distribution," in *Computer Aided Chemical Engineering*. Elsevier, 2018, vol. 43, pp. 1117–1122.

[23] M. J. Tenny and J. B. Rawlings, "Efficient moving horizon estimation and nonlinear model predictive control," in *Proceedings of the 2002 American Control Conference (IEEE Cat. No. CH37301)*, vol. 6. IEEE, 2002, pp. 4475–4480.

[24] B. Koletzko et al, "Guidelines on paediatric parenteral nutrition: 5. Carbohydrates," *Journal of Pediatric Gastroenterology & Nutrition*, vol. 41, no. Supplement 2, pp. S28–S32, Nov. 2005.

[25] K. D. Benam et al., "A nonlinear state observer for the bi-hormonal intraperitoneal artificial pancreas," in *2022 44th Annual International Conference of the IEEE Engineering in Medicine & Biology Society (EMBC)*. IEEE, 2022, pp. 171–176.

[26] C. Rao et al., "Constrained state estimation for nonlinear discrete-time systems: Stability and moving horizon approximations," *IEEE transactions on automatic control*, vol. 48, no. 2, pp. 246–258, 2003.

[27] I. Y. Gejadze et al., "Hessian-based covariance approximations in variational data assimilation," *Russian Journal of Numerical Analysis and Mathematical Modelling*, vol. 33, no. 1, pp. 25–39, 2018.